Geovisualization of Mercury Sediment Contamination in Lake Ontario

Geovisualisierung von Quecksilber-Kontamination in den Sedimenten des Ontariosees

K. Wayne Forsythe[1], Chris H. Marvin[2], Debbie A. Burniston[3], Michael W. MacDonald[1], James P. Watt[4]

[1]Department of Geography and Environmental Studies, Ryerson University · forsythe@geography.ryerson.ca
[2]Aquatic Contaminants Research Division, Environment and Climate Change Canada
[3]Water Quality Monitoring and Surveillance Division, Environment and Climate Change Canada
[4]Jacobs Engineering Group

Abstract: Geovisualization of 1968 and 1998 mercury surficial sediment concentrations was enhanced through the use of three-dimensional "3D" bathymetry data. Kriging was performed on the concentration values to create two-dimensional "2D" representations of the lake-bottom sediment surfaces. These were then integrated with the bathymetry data. The 3D representations provide much more insight to the actual range of concentration values and the location of heavily contaminated areas. Deep lake basins and proximity to current and former industrial areas, along with water inflow zones were identified as problem localities. The results can be useful in the planning of future sediment surveys and can also provide information for the prioritization of sediment quality assessment programs.

Keywords: Mercury, contaminated sediments, 3D geovisualization, bathymetry, Lake Ontario

Zusammenfassung: *Die Geovisualisierung der Messung der Quecksilber-Kontamination von 1968 und 1998 in den Sedimenten des Ontariosees wurden durch die Verwendung von 3D Bathymetriedaten deutlich verbessert. Dabei wurde Kriging als räumliches Interpolationsverfahren verwendet um 2D Karten des Seebodensedimentes zu generieren und schlussendlich mit den 3D Bathymetriedaten zu verknüpfen. Diese 3D Visualisierung zeigt einen wesentlich erhöhten Informationsgehalt in punkto der Konzentrationswerte von Quecksilber in den schwer belasteten Gebieten. Höhere Konzentrationen wurden vor allem in der Nähe von tieferen Seebecken, traditionellen Industriegebieten und in der Nähe von Gewässerzuflüssen gefunden. Die Resultate können in weiterer Folge für die zukünftige Planung der Sedimentbeprobung und deren Untersuchung verwendet werden. Ebenso können sie zur Prioritätensetzung bei der Verbesserung der Sedimentqualitätsprogramme dienen.*

Schlüsselwörter: *Quecksilber, Sedimentkontamination, 3D Geovisualisierung, Bathymetrie, Ontariosee*

1 Introduction

It is estimated that 20% of the world's fresh water is contained within the Laurentian Great Lakes of North America. There are five main lakes (Superior, Michigan, Huron, Erie and Ontario) within the Great Lakes Basin (Fig. 1). The smallest and second in terms of depth is Lake Ontario (Jakubek & Forsythe, 2004; Anderson et al., 2018). It is located at the lower end of the lake/river system that is eventually drained through the St. Lawrence River. The water in the lake comes primarily from the Niagara River that connects upstream to Lake Erie. The Welland Canal also provides water inflow from Lake Erie. Within the Canadian

AGIT – Journal für Angewandte Geoinformatik, 5-2019, S. 348-359. © Wichmann Verlag, VDE VERLAG GMBH · Berlin · Offenbach. ISBN 978-3-87907-669-7, ISSN 2364-9283, eISSN 2509-713X, doi:10.14627/537669033.

Province of Ontario, the Credit, Don, and Trent Rivers along the northern shore provide additional water inputs. In the American State of New York on the southern shore, the Genesee, Oswego, and Black Rivers supplement water supply to the lake (LOLMP, 1998; Jakubek & Forsythe, 2004).

Fig. 1: Location of Lake Ontario in the Laurentian Great Lakes of North America (Source: modified after Forsythe & Watt, 2006; World Atlas, 2006)

A mini-box sediment core sampling procedure was utilized to collect surficial sediment samples in 1998. The survey and associated procedures were designed for clay, sand, silt or mud acquisition. These are considered to be finer grained sediments. All of the samples were frozen after being acquired and then analyzed using standard laboratory procedures. Only the top three centimetres of the sediment column were examined (Marvin et al., 2002). The procedures were aimed at identifying the concentrations of persistent organic pollutants and metals. In addition, particle size characterization and nutrients analyses were undertaken (Marvin et al., 2002). This research also examined mercury (Hg) distribution for 1968 when a historical sediment survey was conducted using similar sampling techniques. The most recent data set is twenty years old and there is a 30-year gap between the two sediments surveys. The time period does, however, coincide with a binational management effort between Canada and the USA to reduce sources of contamination thus making the two comprehensive lake-wide surveys a valuable source of information.

The Canadian Environmental Protection Act identifies mercury as a persistent toxic substance (CCME, 1999; Forsythe et al., 2016b; Mitchell et al., 2018). This is due to its ability to bioaccumulate. It can also reduce fertility and hinders biological development. Deadly consequences for marine and human life can occur when concentrations are high (CCME, 1999; Forsythe et al., 2016b; Mitchell et al., 2018). Throughout this article, reference will be made to the Threshold Effect Level (TEL) and the Probable Effect Level (PEL). These refer to a set of guidelines established by the Canadian Council of Ministers of the Environment (CCME, 1999). The TEL is defined as the concentration below which adverse biological effects are expected to occur rarely while the PEL is defined as the concentration level above which adverse biological effects are expected to occur frequently (Jakubek & Forsythe, 2004; Forsythe et al., 2016b). A range of studies have utilized the TEL and PEL when sediment quality in various water bodies has been assessed in the Great Lakes region (Forsythe et al., 2004; Forsythe & Marvin, 2005; Forsythe et al., 2006; Forsythe & Marvin, 2009; Forsythe et al., 2010; Gawedzki & Forsythe, 2012; Forsythe et al., 2013; Forsythe et al., 2015; Mitchell et al., 2018; Mitchell et al., 2019). The TEL and PEL for mercury are 0.17 µg/g and 0.486 µg/g respectively (Forsythe & Marvin, 2005; Forsythe et al., 2016b).

Mercury occurs naturally in the environment and can be found in most rocks and soils (LOLMP, 1998; Forsythe et al., 2004; Jakubek & Forsythe, 2004; Perlinger et al., 2018). It is a major constituent in batteries and can be found in medical/dental products and thermometers. It is also used in the electrical industry. Waste incineration results in atmospheric emissions that result in mercury inputs into the environment. Historical manufacturing and industrial processes have also resulted in additional inputs into the Great Lakes (LOLMP, 1998; Forsythe et al., 2004; Jakubek & Forsythe, 2004; Forsythe & Marvin, 2005; Forsythe & Marvin, 2009; Mitchell et al., 2018; Perlinger et al., 2018).

2 Methodology

2.1 Interpolation

The kriging spatial interpolation results were generated from the sediment sample points from the 1968 (Fig. 2) and 1998 (Fig. 3) using the Geostatistical Analyst extension of the ArcGIS software package. For 1968 and 1998, the parameters were determined through experimentation. Interpolated surfaces allow for the generation of lake-wide mercury contaminant distribution patterns. Ordinary kriging was chosen as it was found to be a robust method for conducting analyses in similar environments (Forsythe et al., 2004; Forsythe & Marvin, 2005; Forsythe et al., 2006; Forsythe & Marvin, 2009; Forsythe et al., 2010; Gawedzki & Forsythe, 2012; Forsythe et al., 2013; Forsythe et al., 2015; Forsythe et al., 2016b; Mitchell et al., 2018; Mitchell et al., 2019). The spherical model provided the best estimates for both years. When setting the parameters, the number of nearest neighbours also needs to be specified. The values were one and five respectively. Log-normalization was unnecessary in both cases. Table 1 outlines the characteristics of the datasets.

Table 1: Mercury data characteristics for 1968 and 1998 (dry weight)

Study Year	Number of Samples	Minimum (µg/g)	Maximum (µg/g)	Average (µg/g)
1968	258	0.03	2.10	0.65
1998	69	0.02	1.38	0.59

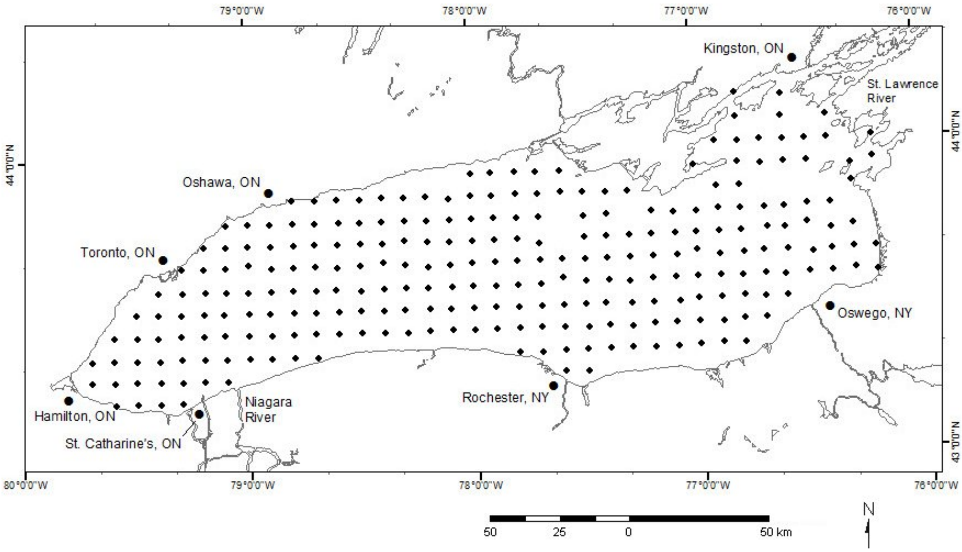

Fig. 2: Lake Ontario 1968 Sediment Survey Sample Points

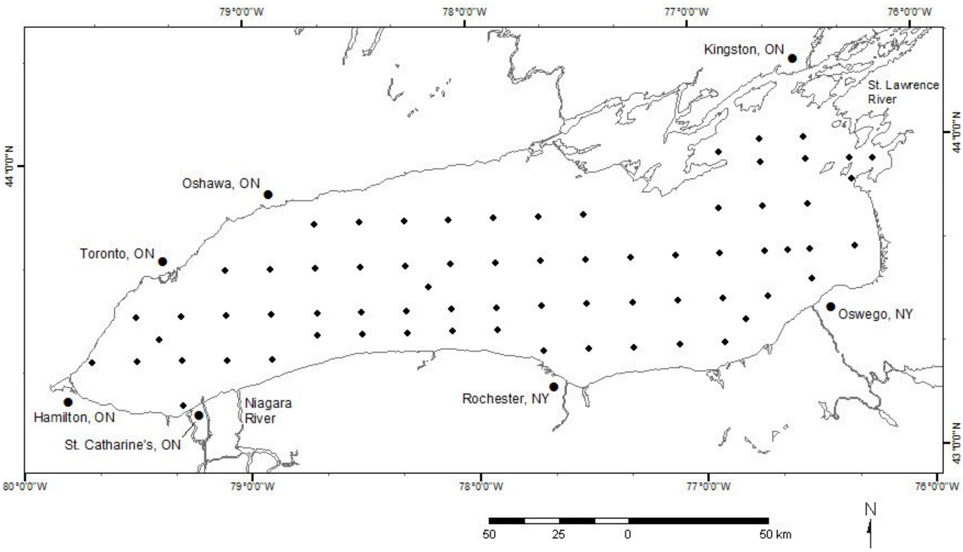

Fig. 3: Lake Ontario 1998 Sediment Survey Sample Points

Although the number of samples acquired in 1998 is much lower than 1968, kriging allows for the surfaces to be directly compared as area estimates. The 1998 estimates may be more generalized however the surfaces are subject to rigorous statistical testing to ensure their validity (Forsythe et al., 2004; Forsythe and Marvin, 2005; Forsythe et al., 2016b). Model error statistics are utilized for determining the accuracy of kriging predictions. Table 2 outlines the values. For a kriging spatial interpolation model to provide accurate estimates and generate meaningful surfaces, the following conditions must be met:

- the Mean Prediction Error (MPE) should be ~0,
- the Average Standard Error (ASE) should be as low as possible (<20),
- and the Standardized Root Mean Square Prediction Error (SRMSPE) should be close to 1 (Forsythe et al., 2004; Forsythe and Marvin, 2005; Forsythe et al., 2016b).

When the SRMSPE is >1, the prediction surfaces are underestimated, while when the value is <1, the estimates are overestimated (Forsythe et al., 2016b; Mitchell et al., 2018). When the statistics of the 1968 and 1998 models are examined, the values can confidently be utilized as they are statistically valid.

Table 2: Kriging Model Error Statistics

Study Year	Model	MPE	ASE	SRMSPE
1968	Spherical	0.0026	0.2656	1.1093
1998	Spherical	0.0121	0.3552	0.9675
Ideal	–	~0.0000	<20.0000	~1.0000

2.2 Visualization

The two-dimensional (2D) kriging estimates (Fig. 4 and Fig. 5) were created within ArcMap, while the three-dimensional (3D – also referred to as 2.5D) geovisualizations were produced using ArcScene. The 3D bathymetry surface has a 90m spatial resolution. It was originally developed by the National Oceanographic and Atmospheric Administration (NOAA 2014).

In order for the variations and undulations in the bathymetry model to be more visible, view settings needed to be employed. This included altering both shadow and depth contrast. The 2D images are viewed from the south while the 3D images were are viewed from the west rather than the traditional southern perspective to ensure the visualization of the largest portion on the lake-bottom. The steep bathymetric drop-off from the southern shoreline into Lake Ontario inhibits full 3D geovisualization of all of the lake-bottom bathymetry features (Forsythe et al., 2016a; Mitchell et al., 2018). Cartographically and visually, the results are optimized as the western viewpoint provides the least obstructed view of the lake-bottom.

3 Results

For 1968 and 1998, the statistics give an indication of the validity of the prediction estimates. A slight under prediction is noted for the 1968 surface due to the SRMSPE value of 1.1093, while a slight overestimate occurs with the 0.9675 value for 1998. Spherical models proved to be the most suitable (of Gaussian, exponential and spherical) models that were examined and mapped. Additional parameters that were arrived at through experimentation include the major and minor search radii. For 1968 the major and minor vales were 50 km and 25 km respectively. For 1998, these values were 100 km and 50 km. In all scenarios, 90 degrees was the search direction. Experimentation was utilized to determine all model parameters with previous research results also influencing the selections.

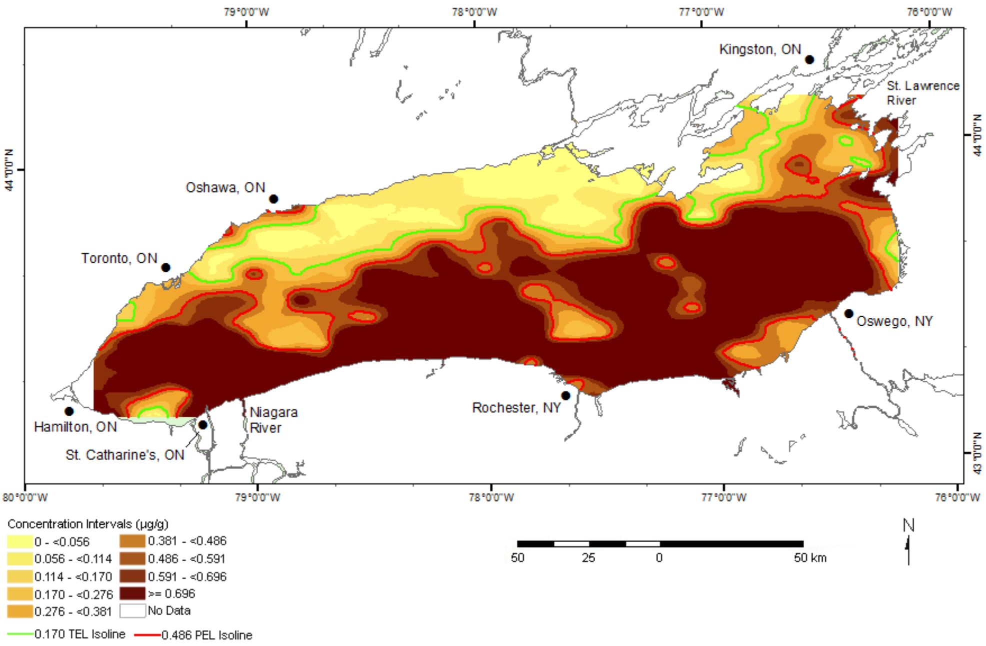

Fig. 4: Lake Ontario Kriged 1968 Mercury Contamination

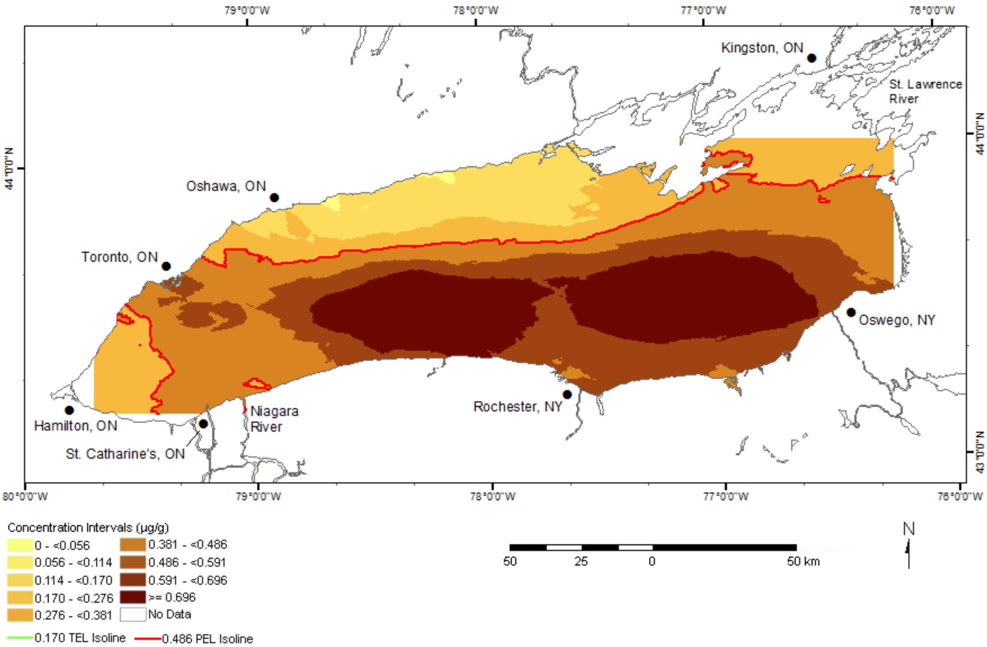

Fig. 5: Lake Ontario Kriged 1998 Mercury Contamination

Knowledge of lake-bottom features (Fig. 6), is useful in assessing the contaminant distribution patterns. The location of underwater sills and depositional basins assists in interpreting the results of the kriging analyses with bathymetric features. Sills are underwater ridge features which act as barriers inhibiting sediment movement. The depositional basins are areas where sediments tend to migrate downward overtime (Forsythe et al., 2004; Forsythe & Marvin, 2005; Forsythe et al., 2010; Forsythe et al., 2016a). Additionally, annualized circulation (Fig. 7) also contributes to sediment distribution patterns, especially the eastward flowing current along the southern shoreline of the lake. Knowledge regarding historical and current industrial and manufacturing sites further assists in interpreting the results. The location of the larger cities related to these types of activities is illustrated in the kriged figures. The Niagara River is also important as it provides the majority of the inflow to Lake Ontario.

Bathymetry data (Fig. 8) are valuable in assessing sediment contamination patterns. Lighter tones in the bathymetry indicate deeper lake areas. When the reverse colour ramp was used, the lake-bottom features were not as visible and this led to poor geovisualization of the data.

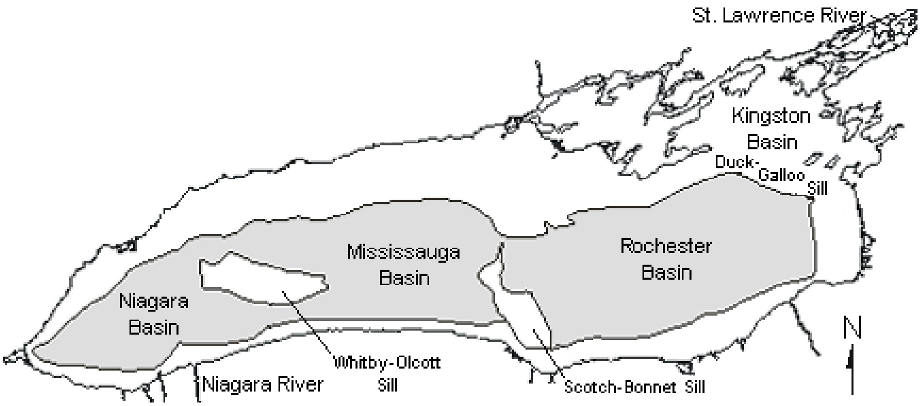

Fig. 6: Lake Ontario bathymetry including major depositional basins, modified after (Marvin et al., 2003; Forsythe et al., 2004)

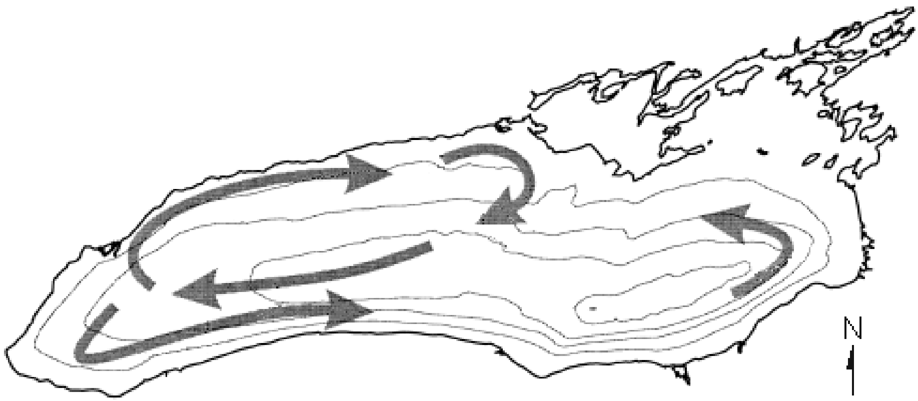

Fig. 7: Annual circulation in Lake Ontario – isobaths every 50 m, modified after (Beletsky et al., 1999; Forsythe et al., 2004)

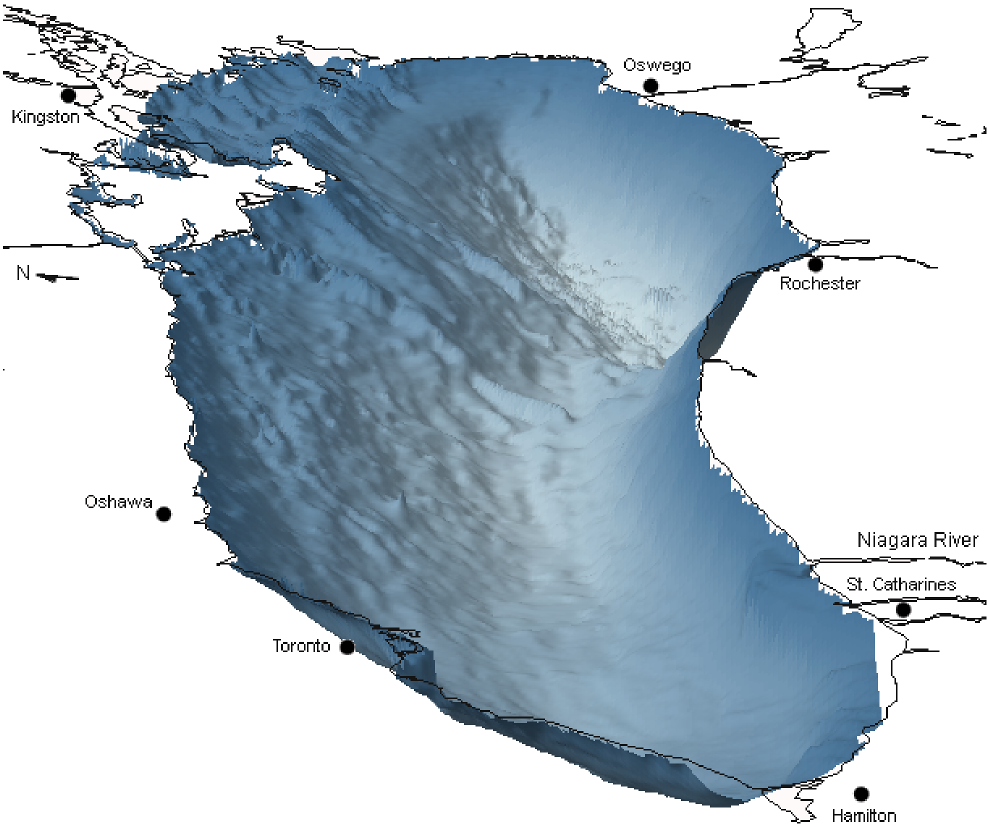

Fig. 8: Bathymetry Data Model for Lake Ontario (west perspective)

Fig. 9 illustrates the 1968 mercury results in 3D. The 1998 mercury data (Fig. 10) were also analyzed using this technique. The sediment distribution patterns are much more visible using this geovisualization technique. The Niagara Basin, Mississauga Basin and the Rochester Basin clearly are areas of higher mercury concentrations in 1968. There are slight interruptions to this pattern due to the location of the Whitby-Olcott Sill and the Scotch-Bonnet Sill in the western and eastern portions of the lake respectively. The Duck-Galloo Sill acts as an impediment to sediment output to the St. Lawrence River in the northeast part of the lake. Mercury concentrations below the TEL are mostly found in shallower sections of the lake near the northern shoreline. The reasons for this include limited manufacturing and industrial development in these areas. In addition, there is a tendency for mercury and other contaminants to migrate downward over time (Forsythe et al., 2016b). The contamination patterns are also better visualized when taking the TEL and PEL isolines into account. The kriged data surfaces are much more interpretable due to the inclusion of the bathymetry data.

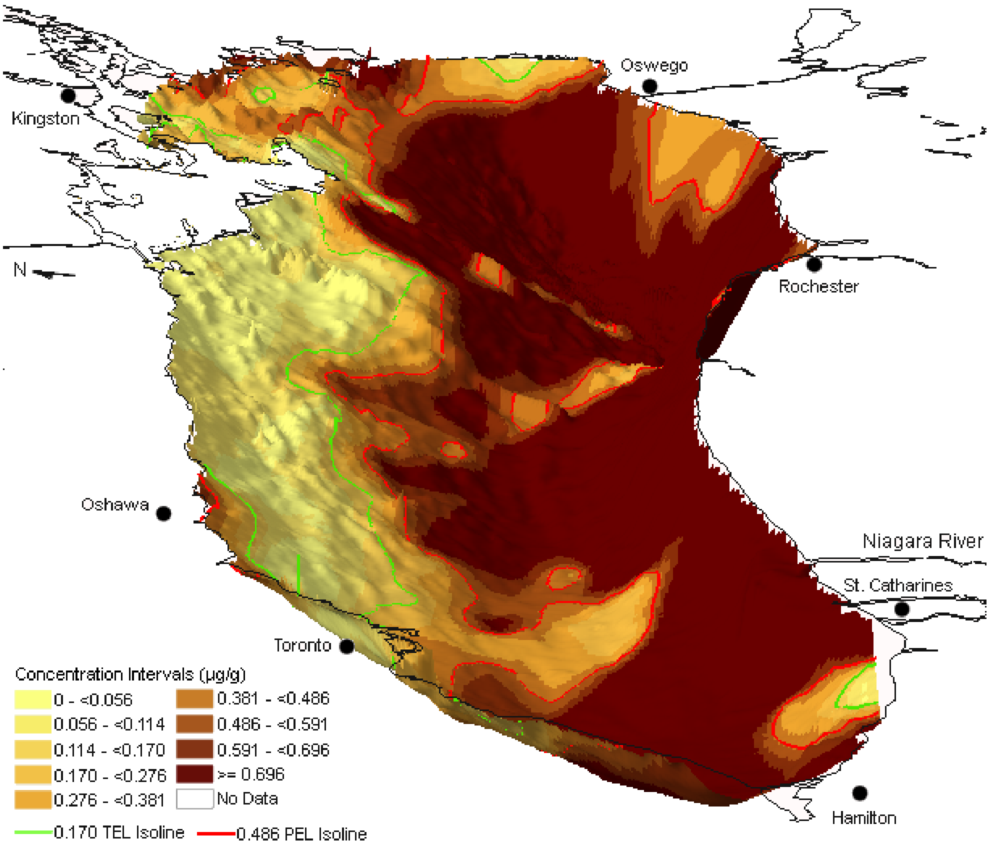

Fig. 9: Lake Ontario Kriged 1968 Mercury Contamination with Bathymetry

For 1998 mercury, the patterns are much more generalized. This may in part be due to having only 69 sample points available compared to 258 in 1968. Noticeable however is the fact that the PEL (or greater) areas have diminished in size and the total concentrations are reduced. It appears that there has been an increase in the areas between the TEL and PEL (especially along the northern shoreline) however this can in part be attributed to the more general prediction surface being produced with fewer points.

In 1968, larger portions of the lake were more polluted. This can especially be seen with respect to the highest PEL category. More points are usually better to perform most spatial interpolation procedures however acquisition of the same set of sample points was not considered in 1998 due to the high cost obtaining and analyzing samples. It was possible to generate lake-wide estimates for both the 1968 and 1998 datasets. The utilization of bathymetry data also allows for a much more detailed analysis of the patterns that were observed and the relationship in many areas between mercury contaminant concentrations, depth, circulation patterns and source areas can be visualized. This could assist in the design of future sediment sampling programs which are challenging to design and costly to implement.

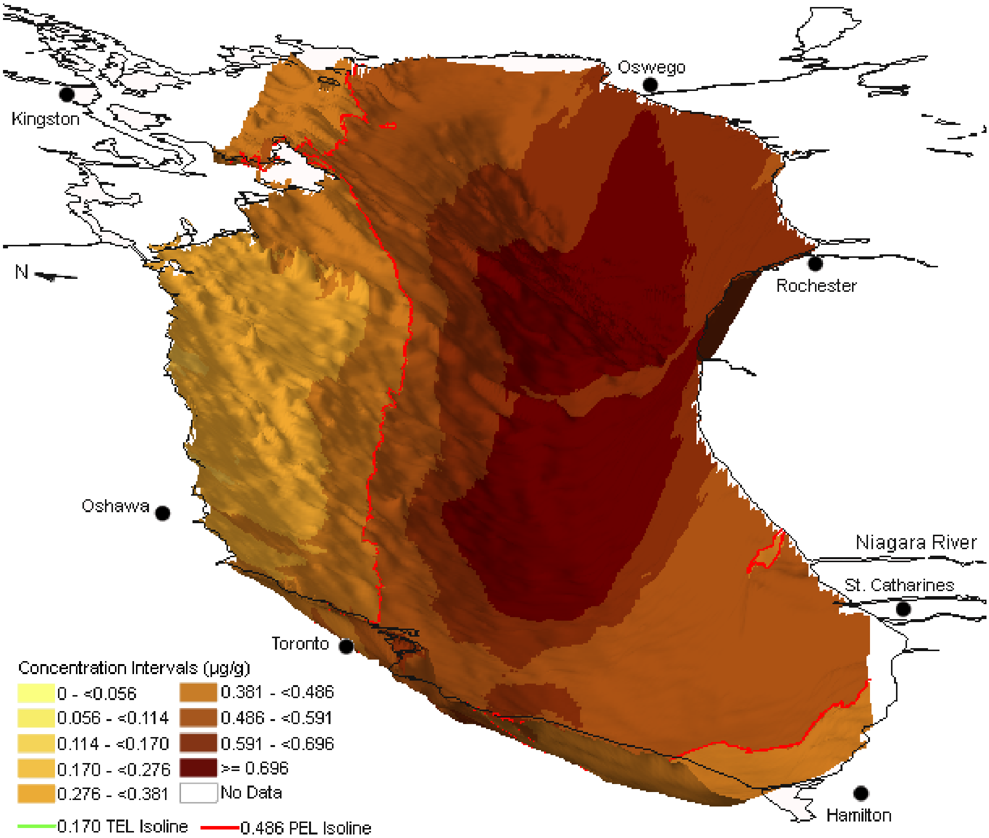

Fig. 10: Lake Ontario Kriged 1998 Mercury Contamination with Bathymetry

4 Conclusions

The kriging interpolation technique results, when combined with bathymetric observations of the lake-bottom, enable the analysis of mercury contaminant distribution. Knowledge of underwater features assisted with the interpretation of the results. It was observed that Lake Ontario had large areas of contamination above the PEL in both years that were analyzed. Pollution levels were lower in 1998 as compared to 1968. An improved understanding of the impact of anthropogenic sources of mercury on open-lake environs was acquired through these analyses. Information that assists in tracking progress in toxic reduction was also obtained, despite the comprehensive lake-wide surveys being conducted in 1968 and 1998. Binational management action does appear to have reduced the concentrations of mercury during a period of cooperative binational management aimed at reducing chemical contamination in Lake Ontario and the other Great Lakes. Pollution controls that have been implemented since the last survey may result in lower mercury contaminant concentrations when future surveys are conducted. The design of those surveys could benefit from an examination of the results in this article.

References

Anderson, E. J., Lang, G., Kelley, J., & Zhang, A. (2018). *Great Lakes Coastal Forecasting System: Next Generation*. Retrieved Feb 7, 2018, from https://www.glerl.noaa.gov/res/Programs/ipemf/GLCFS_nextgen.html.

Beletsky D., Saylor J. H., & Schwab D. J. (1999). Mean circulation in the Great Lakes. *Journal of Great Lakes Research*, *25*(1), 78–93.

CCME – Canadian Council of Ministers of the Environment (1999). *Canadian environmental quality guidelines*. Winnipeg, MB, Canada: Canadian Council of Ministers of the Environment.

Forsythe, K. W., Dennis, M., & Marvin, C. H. (2004). Comparison of Mercury and Lead Sediment Concentrations in Lake Ontario (1968-1998) and Lake Erie (1971-1997/98) using a GIS-based Kriging Approach. *Water Quality Research Journal of Canada*, *39*(3), 190–206.

Forsythe, K. W., Gawedzki, A., Rodriguez, P. S., Irvine, K. N., & Perrelli, M. F. (2013). Geospatial Estimation of Mercury Contamination in Buffalo River Sediments. *Soil and Sediment Contamination An International Journal*, *22*(5), 521-531, doi:10.1080/15320383.2013.750266.

Forsythe, K. W., Irvine, K. N., Atkinson, D. M., Perelli, M., Aversa, J. M., Swales, S. J., Gawedzki, A., & Jakubek, D. J. (2015). Assessing lead contamination in Buffalo River sediments. *Journal of Environmental Informatics*, *26*(2), 106–111, doi:10.3808/jei.201500300.

Forsythe, K. W., & Marvin, C. H. (2005). Analyzing the spatial distribution of sediment contamination in the Lower Great Lakes. *Water Quality Research Journal of Canada*, *40*(4), 389–401.

Forsythe, K. W., & Marvin, C. H. (2009). Assessing Historical versus Contemporary Mercury and Lead Contamination in Lake Huron Sediments. *Aquatic Ecosystem Health & Management*, *12*(1), 101–109, doi:10.1080/14634980802690873.

Forsythe, K. W., Marvin, C. H., Mitchell, D. E., Aversa, J. M., Swales, S. J., Burniston, D. A., Watt, J. P., Jakubek, D. J., McHenry, M. H., & Shaker, R. R. (2016a). Utilization of bathymetry data to examine lead sediment contamination distributions in Lake Ontario. *AIMS Environmental Science*, *3*(3), 347–361, doi:10.3934/environsci.2016.3.347.

Forsythe, K. W., Paudel, K., & Marvin, C. H. (2010). Geospatial analysis of zinc contamination in Lake Ontario sediments. *Journal of Environmental Informatics*, *16*(1), 1–10.

Forsythe, K. W., Marvin, C. H., Valancius, C. J., Watt, J. P., Aversa, J. M. Swales, S. J., Jakubek, D. J., & Shaker, R. R. (2016b). Geovisualization of Mercury Contamination in Lake St. Clair Sediments. *Journal of Marine Science and Engineering*, *4*(19), 1–10. doi:10.3390/jmse4010019.

Forsythe, K. W., & Watt, J. P. (2006). Using Geovisualization to Assess Sediment Contamination in the "Sixth" Great Lake. *Proceedings of the 18th Symposium for Applied Geographic Information Processing, AGIT XVIII*, Salzburg, Austria, July 5-7, 2006; Strobl, J., Blaschke, T., & Griesebner, G. (Eds.) (pp. 161–170). Heidelberg: Wichmann.

Gawedzki, A., & Forsythe, K. W. (2012). Assessing anthracene and arsenic contamination within Buffalo River sediments. *International Journal of Ecology, 2012,* doi: 10.1155/2012/496740.

Jakubek, D. J., & Forsythe, K. W. (2004). A GIS-based kriging approach for assessing Lake Ontario sediment contamination. *The Great Lakes Geographer*, *11*(1), 1–14.

LOLMPL (1998). *Lake Ontario Lakewide Management Plan*. Retrieved Feb 7, 2018, from https://www.epa.gov/greatlakes/lake-ontario.

Marvin, C. H., Charlton, M. N., Reiner, E. J., Kolic, T., MacPherson, K., Stern, G. A., Braekevelt, E., Estenik, J. F., Thiessen, L., & Painter, S. (2002). Surficial sediment contamination in Lakes Erie and Ontario: A comparative analysis. *Journal of Great Lakes Research*, *28*(3), 437–450.

Marvin, C. H., Charlton, M. N., Stern, G. A., Braekevelt, E., Reiner, E. J., & Painter, S. (2003). Spatial and temporal trends in sediment contamination in Lake Ontario. *Journal of Great Lakes Research*, *29,* 317–331.

Mitchell, D. E., Forsythe, K. W., Marvin, C. H., & Burniston, D. A. (2018). Assessing Statistical and Spatial Validity of Sediment Survey Design and Sampling Densities: Examples from Lake Erie. *Water Quality Research Journal*, *53*(3), 118–132. doi:10.2166/wqrj.2018.029.

Mitchell, D. E., Forsythe, K. W., Marvin, C. H., & Burniston, D. A. (2019). Temporal Trends and Origins of Lake Erie Cadmium Contamination in Relation to Sediment Substrate Type Using Multivariate Kriging Analyses. *International Journal of Geospatial and Environmental Research*, *6*(1), Article 3, 1–21.

NOAA – National Oceanographic and Atmospheric Administration (2014). *Great Lakes bathymetry*. Retrieved Feb 7, 2018, from https://www.ngdc.noaa.gov/mgg/greatlakes/greatlakes.html.

Perlinger, J. A., Urban, N. R., Giang, A. et al. (2018). Responses of deposition and bioaccumulation in the Great Lakes region to policy and other large-scale drivers of mercury emissions. *Environmental Science: Processes & Impacts*, *20*, 195–209.

World Atlas (2006). *The Great Lakes*. Retrieved Apr 13, 2019, from http://worldatlas.com/webimage/countrys/namerica/greatlk.htm.